ATMOSPHERIC CIRCULATION CHANGES DUE TO INCREASED GREENHOUSE WARMING AND ITS IMPACT ON SEASONAL RAINFALL IN THE MEDITERRANEAN AREA

JUCUNDUS JACOBEIT*

Geographical Institute, University of Würzburg

Summary: *Geopotential height data from the coupled OAGCM of Hamburg (ECHAM/LSG) with T21-resolution are used for the last 10 years of a transient simulation 100 years into the future according to IPCC-Scenario A ("business as usual") and for the corresponding time span from the control run. Principal components analyses have been performed for seasonal months on both hemispheres. The main signals of change due to enhanced greenhouse warming occur during the winter seasons: a shift towards meridional circulation patterns on the southern hemisphere, an increase in PNA-like patterns and in the positive phase of the NAO on the northern hemisphere. Applying statistical downscaling techniques in order to assess the impact of these circulation changes on seasonal rainfall at 91 Mediterranean stations, we get common increases of rainfall in the northern part and prevailing decreases elsewhere with a strengthening tendency towards the south.*

1. INTRODUCTION

Climatic changes due to enhanced greenhouse warming mostly are discussed in terms of basic elements (e.g. temperature or precipitation), whereas it is the atmospheric circulation whose response to the global forcing by increasing concentrations of atmospheric greenhouse gases leads to the actual arrangement of climate change implying spatial differences in atmospheric flow characteristics and thus very crucial changes of climate also on a regional scale. In order to study such circulation changes we have used some output data from a coupled OAGCM which has performed several time-dependent simulations up to 100 years into the future (*Cubasch et al., 1992*). Selecting the last 10 years of an integration according to IPCC-Scenario A ("business as usual", see *Houghton et al., 1990*), we intend to find out whether there is a significant shift in atmospheric circulation patterns due to continuously and unrestrictedly increasing greenhouse gases in the atmosphere. Since model bias has to be considered, these 10 scenario years are not compared with recent observations but with the corresponding time span from the model control run which likewise represents a nearly present level of greenhouse gases in the atmosphere.

These results may indicate the general direction of large-scale circulation changes, but they still do not allow to estimate the corresponding regional changes in climate at higher spatial resolution. *Grotch and MacCracken (1991)* even point to deviations (for seasonal periods) between projected changes from different models of the same order of magnitude as the perturbations themselves. Therefore, in a second step, empirical relations between regional climate data (in this case: monthly rainfall at 91 Mediterranean stations) and the large-scale circulation in the Atlantic/European/Northafrican area have been derived from recent observations in order to transfer these relations to conditions of a global warming by entering the model circulation mentioned above instead of the presently observed circulation. This downscaling technique has been successfully applied in various regional climate change studies (e.g. by *v. Seggern (1992)*, *v. Storch et al. (1993)*,

* Address: Am Hubland, D – 97074 Würzburg, FRG

Jakob (1993), Burkhardt and Metz (1994) or *Gyalistras et al. (1994)*) and will be used in this paper to estimate regional rainfall changes due to enhanced global greenhouse warming, focusing on an area of high climatic sensitivity like the Mediterranean region with its alternating wet and dry seasons. Shifts in general circulation patterns analysed before are expected, in conclusion, to enlighten the dynamical background for this regional scenario.

2. DATA BASE

Three different data sets have been used for this study:

- Daily grids of sea-level pressure (SLP), 500 and 300 hPa geopotential heights (GP500 and GP300) from the last 10 years of a transient simulation 100 years into the future according to IPCC scenario A by the T21 version of the coupled OAGCM of Hamburg (ECHAM/LSG), including the corresponding data from the control run (source: DKRZ Hamburg). The atmospheric component of the model consists of a modified low-resolution version of the ECMWF-GCM, the oceanic component ("Large-Scale Geostrophic") also includes the deep sea circulation and is coupled syncronously to the atmospheric part (see *Cubasch et al., 1992*). In the meanwhile there are advanced model versions concerning both, improved model physics and increased spatial resolution. Until now, however, no other transient simulations up to 100 years into the future than those from the initial model have been available.
- Daily grids of SLP and GP500 (spatial resolution $5° \times 5°$) for the northern hemisphere during the period 1947 – 1987 (source: NCAR).
- Monthly precipitation data for the same period (source: Climatic Research Unit, University of East Anglia) including 91 Mediterranean stations outside the Iberian peninsula (analysed by von *Storch et al. (1993)* with respect to winter rainfall). Algeria and parts of the eastern Mediterranean have not been included due to data problems.

3. HEMISPHERIC CIRCULATION CHANGES

3.1 Methods

Monthly averaged GP500 grids from the last decade of the scenario-A-integration and the control run have been submitted to T-mode principal components analyses, separately for each season on both hemispheres between 20° and 70° of latitude. Basic circulation patterns are obtained as standardized scores, corresponding time coefficients as orthogonally rotated loadings. Differences in circulation between scenario A and control run subsets are examined by comparisons of the standardized variances explained by these circulation patterns within the two subsets, statistical significance of differences is checked according to Mann-Whitney's test for independent samples.

Furthermore, general circulation intensities are estimated by means of calculations (on a monthly averaged basis) of hemispheric meridional thickness gradients between subtropical and subpolar latitudes within the lower (500/1000 hPa layer) and the upper troposphere (300/500 hPa layer). Standardized deviations of these thickness gradients will be compared between scenario A and control run subsets including once more Mann-Whitney tests for statistical significance.

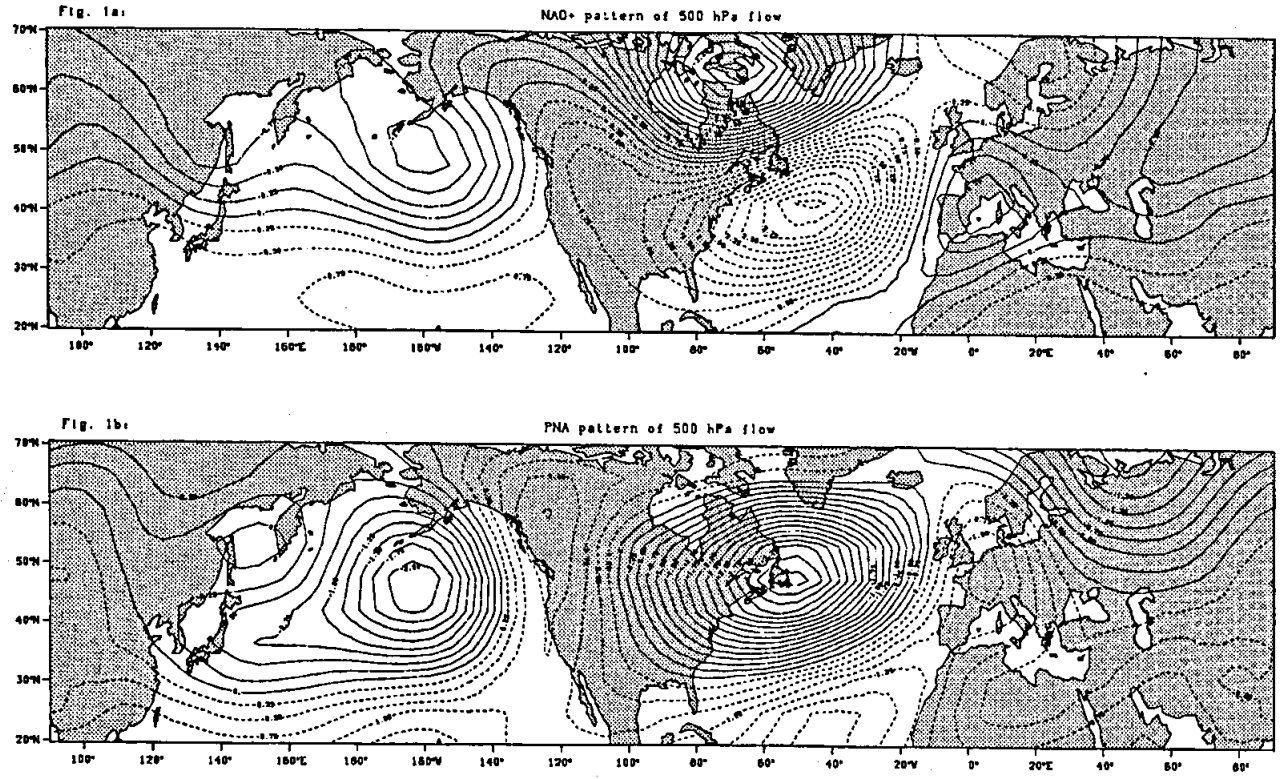

Fig. 1. Standardized scores (> 0 dashed) of selected T-mode principal components derived from 500 hPa geopotential height grids originating from ECHAM/LSG scenario A and control runs (wintermonths of model years 91 - 100). The two selected patterns are those with increased explained variances within the scenario A subset.

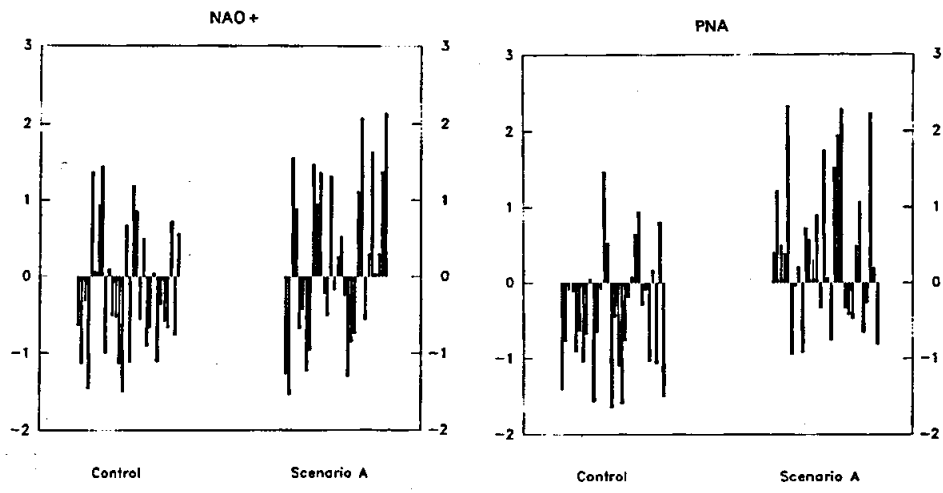

Fig. 2. Standardized variances of northern hemispheric 500 hPa geopotential height grids explained by NAO+ and PNA patterns within control and scenario A subsets (wintermonths of ECHAM/LSG model years 91-100)

3.2 Results

The main circulation differences between control and scenario A occur during the winter seasons: there are, on both hemispheres, some of the resulting circulation patterns with significantly differing variances explained within the two subsets, thus indicating shifts between these patterns due to increased global greenhouse warming.

The analysis for northern hemispheric winter leads to 4 basic circulation patterns (explained variance: 97·8%), one of them (a wave pattern of wave number 3) without substantial differences in standardized variances between the two subsets. Another pattern which more or less is representing negative modes of the North-Atlantic Oscillation (NAO), explains significantly (99·9% level) less variance within the scenario subset compared to the control subset (*Jacobeit, 1994c*). Fig. 1 shows the remaining patterns which gain extended importance under scenario A conditions (Fig. 2): increases in explained variances still remain at a rather low level of significance (90%) for the positive phase of the NAO, but become highly significant (99·9%) for the remaining pattern which clearly resembles to the well-known Pacific-North-American pattern (PNA). Compared to PNA modes derived from recent data based on observations (*Jacobeit, 1993*), this pattern additionally shows internal modifications like the expansion and deepening of the eastern American cyclonic centre or the anticyclonic wave shifted from the mid-Atlantic towards western and central Europe. The latter might be due to model bias (*Roeckner et al., 1992*), but remarkably the recent trends (1967 – 1989) of geostrophic winds at the 500 hPa level reveal a quite similar pattern during wintertime (*Flohn et al., 1992*). Moreover, general shifts in circulation patterns between control and scenario A as mentioned above have

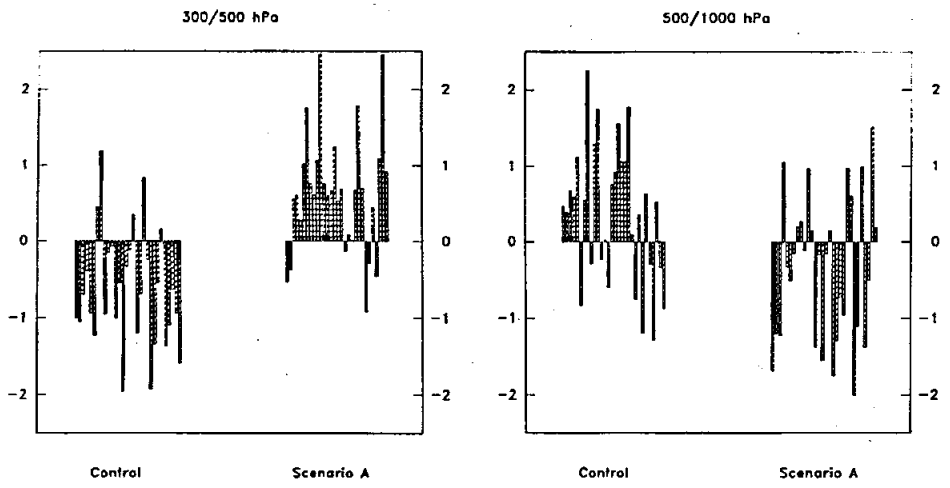

Fig. 3. Standardized values of northern hemispheric meridional gradients of 300/500 hPa and 500/1000 hPa thicknesses between subtropical and subpolar latitudes within control and scenario A subsets (wintermonths of ECHAM/LSG model years 91 – 100).

proved to take place already during recent decades of observation: increases, during wintertime, in PNA patterns (*Jacobeit, 1993; Wallace and Zhang, 1993*) as well as in intensity of the baroclinic upper westerlies (*Flohn et al., 1990*) and in frequency of zonalized large-scale weather patterns of the Atlantic/European region (*Bardossy and Caspary, 1990*), reflecting positive modes of the NAO becoming more important.

Thus, for wintertime, recent trends as well as model results point to similar developments of circulation in response to global warming: enhanced cyclonic activity in the Northern Pacific area and around the eastern part of North America, growing anticyclonic influence above the northwestern region of this continent, a stronger zonalization of the North Atlantic circulation with reduced European trough activity and possibly increasing high pressure influence above the western part of Europe.

These circulation changes are working on the background of changing meridional temperature gradients (expressed in terms of thickness gradients of relative topographies), comparing control and scenario A subsets (Fig. 3): during winter, we get decreasing gradients with enhanced greenhouse warming in the lower troposphere (due to the ice-albedo-feedback in higher latitudes), but increasing gradients in the upper troposphere (due to the H_2O-feedback in lower latitudes). These different changes may account for the simultaneous increases in PNA and NAO+ patterns described above.

During southern hemispheric winter we get increasing gradients with enhanced greenhouse warming not only in the upper, but also in the lower troposphere (*Jacobeit, 1994c*). As a result, critical instability thresholds for large-amplitude wave formations might be exceeded more frequently: in fact, among 5 basic circulation patterns resulting from principal components analysis, there is a zonal one which decreases, and a meridional one which increases in explained variances (95% level of significance)

comparing the scenario subset with the control subset (*Jacobeit, 1994c*). Thus, more regional differences in climate caused by large-scale circulations may be expected for the southern hemisphere under conditions of an enhanced greenhouse warming.

4. REGIONAL RAINFALL CHANGE ESTIMATES

4.1 Methods

In order to derive empirical relations between the large-scale circulation and Mediterranean rainfall, approximations of the geostrophic zonal and meridional component and of the relative vorticity have been calculated from the GP500 grids. These variables as well as the original SLP and GP500 grids have been submitted to S-mode principal components analyses within the Atlantic/European/Northafrican region (20 – 70°N, 50°W – 40°E) in order to represent the temporal behaviour of its circulation by scores of a limited number of principal components explaining most of the total variances (between 66% and 89%). This step includes observed and simulated data and has been carried out separately for the seasons except summer when widespread areas of the Mediterranean region experience quite dry conditions. Fig. 4 gives an example of the spatial pattern of principal components (orthogonally rotated GP500 loadings for the winter season) summarizing just the highest values >= 0·7 for all of the extracted principal components. Obviously there is a clear-cut organization into distinct centres of action. Similar results are obtained for the other variables and seasons, summing up to a number between 54 and 63 of principal components for each season which further are used as influencing variables for the establishment of relations between large-scale circulation and Mediterranean rainfall.

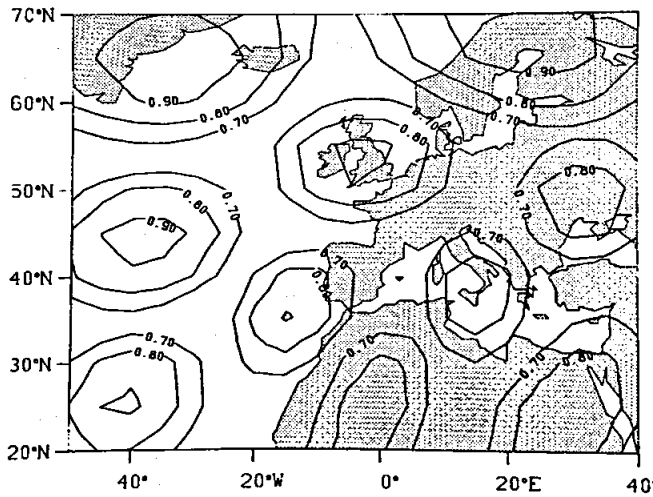

Fig. 4. Spatial pattern of loadings >= 0·7 of the first 10 S-mode principal components derived from Atlantic/European 500 hPa geopotential height grids (wintermonths of the years 1947 – 1987 (covered by observation) and of ECHAM/LSG model years 91 – 100).

On a monthly basis, multiple regression analyses for each season have been performed between the time coefficients of these principal components from the observation period and the corresponding Mediterranean rainfall data. As pointed out by *Wigley et al. (1990)*, there are quite large spatial differences in the amount of local climate variance that can be explained by large-scale information, and therefore multiple regression equations have been established with rainfall data factorized by S-mode principal components, too (based on a division of rainfall stations into 4 regional subgroups: Italy and the adjacent Westmediterranean area, Greece and western Turkey, Morocco, and the Mediterranean band of northern Africa further east). With a confidence level of 95% for regression coefficients we get a number between 3 and 10 (out of 54 to 63) of the influencing variables which enter the resulting equations. Multiple correlation coefficients for the individual rainfall factors range between 0·32 and 0·81 indicating considerable parts of total variances that cannot be explained by the large-scale circulation. Since all of the rainfall factors contribute (with varying proportions) to the original variances of the observed data, the latter are reproduced reasonably well by the derived regression models (best approximations at the western margin (Morocco) of the study area).

Replacing the atmospheric time coefficients from the observation period by those from the simulation period (model years 91 – 100) finally leads to empirical assessments of Mediterranean rainfall changes due to enhanced global greenhouse warming. These assessments directly apply to the regional rainfall factors being subsequently retransformed into estimations for the individual rainfall stations.

4.2 Results

Resulting rainfall changes for the individual seasons are shown *by Jacobeit (1994a and 1994b)*, Fig. 5 gives the overall picture for the whole rainy period (autumn, winter, spring). The classified values (10%-intervals in relation to the observed mean values) show common increases in the northern part and prevailing decreases elsewhere with rising amounts, on average, towards lower latitudes. The striking exception in northern Tunisia might result from reinforced cut-off cyclones enhancing daily rainfall intensity and efficiency of extreme rainfall events even for the case of reduced rainfall frequency (*Gordon et al., 1992*). The northern Mediterranean rainfall increases are higher and more widespread in winter (*Jacobeit, 1994a*), but nearly disappear in autumn (*Jacobeit, 1994b*). These estimated changes are in general agreement with completely independent assessments by *Schönwiese and Birrong (1990)* based on empirical models with external forcings.

From the viewpoint of statistics the estimated rainfall changes still are insignificant in most cases. It is only in northern Sicily during autumn that the signal-to-noise ratio exceeds the 95% confidence level, ratios greater than 1·0 sometimes still occur at scattered places (preferably in northwestern Turkey, southern France and Morocco). Nevertheless, the estimated losses which partly exceed a 30% value in some regions, would mean – in case of realization – a substantial worsening of the regional water budgets.

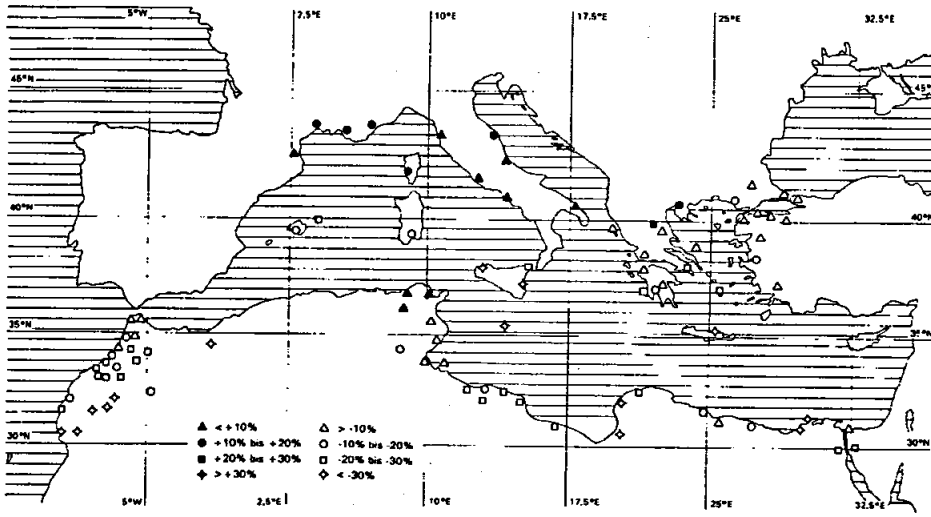

Fig. 5. Estimated changes of Mediterranean rainfall in the rainy period (autumn, winter, spring) due to enhanced greenhouse warming according to IPCC scenario A. Seasonal averaged percentages are derived for ECHAM/LSG model years 91 – 100 and refer to the observed mean values 1947 – 1987.

5. CONCLUSION

This latitudinal pattern of different rainfall changes in the Mediterranean area might be explained by large-scale circulation changes discussed above: the intensified flow resulting from increased NAO values could cause more rainfall in the northern part (especially in winter) whereas the reduced European trough activity concomitant with marked increases in PNA-like patterns would lead to decreased rainfall in the lower latitudes of the Mediterranean area (*Jacobeit, 1994c*). These results, of course, depend on global climate model's qualities, and the earlier version of the ECHAM GCM whose transient simulation output has been used in this study, still suffers from some major deficiencies (e.g. underestimations of the low-frequency variability, of the Northern Atlantic baroclinic activity, of the southern hemispheric circulation intensity, see *Roeckner et al., 1992*). Thus, further confirmation is required from analyses of time-dependent output data from advanced and more sophisticated models.

References

Bardossy, A. & H.J. Caspary (1990): Detection of climate change in Europe by analyzing European atmospheric circulation patterns from 1881 to 1989. *Theoretical and Applied Climatology*, **42**, 155 – 167.

Burkhardt, U. & W. Metz (1994): Interpretation eines ECHAM3/T42-Experimentes in Hinsicht auf den Niederschlag im Alpenraum. *PIK Reports*, **1**, 27 – 29.

Cubasch, U. et al. (1992): Time-dependent Greenhouse Warming Computations With a Coupled Ocean-Atmosphere Model. *Climate Dynamics*, **8**, 55 – 69.

Flohn, H. et al. (1990): Recent changes of the tropical water and energy budget and of mid-latitude circulations. *Climate Dynamics*, **4**, 237 – 252.

Flohn, H. et al. (1992): Water vapour as an amplifier of the greenhouse effect: new aspects. Meteorologische Zeitschrift, *N.F.* **1**, 122 – 138.

Gordon, H.B. et al. (1992): Simulated Changes in Daily Rainfall Intensity Due to the Enhanced Greenhouse Effect: Implications For Extreme Rainfall Events. *Climate Dynamics*, **8**, 83 – 102.

Grotch, S.L. & M.C. MacCracken (1991): The Use of General Circulation Models to predict Regional Climatic Change. *Journal of Climate*, **4**, 286 – 303.

Gyalistras, D. et al. (1994): Linking GCM-simulated climatic changes to ecosystem models: case studies of statistical downscaling in the Alps. *Climate Research*, **4**, 167 – 189.

Houghton, J.T. et al., eds. (1990): Climate Change. The IPCC Scientific Assessment. Cambridge Univ. Press, 356 pp.

Jacobeit, J. (1993): Regionale Unterschiede im atmosphärischen Zirkulationsgeschehen bei globalen Klimaveränderungen. *Die Erde*, **124**, 63 – 77.

Jacobeit, J. (1994a): Empirische Abschätzungen zur Änderung des Winterniederschlags im Mittelmeerraum bei anthropogen verstärktem Treibhauseffekt. *PIK Reports*, **1**, 117 – 121.

Jacobeit, J. (1994b): Empirical estimations of Mediterranean rainfall changes in the transitional seasons due to enhanced greenhouse warming. In: Brazdil, R. & M. Kolar (Eds.): Contemporary Climatology. Brno, 266 – 271.

Jacobeit, J. (1994c): Atmosphärische Zirkulationsveränderungen bei anthropogen verstärktem Treibhauseffekt – jahreszeitliche Analysen in den Außertropen beider Hemisphären auf der Basis von Ausgabedaten globaler Klimamodellsimulationen. *Würzburger Geographische Manuskripte*, **34**, 101 pp.

Jakob, Ch. (1993): Temperature Trends over Europe Downscaled from a GCM-Experiment. Spezialarbeiten aus der Arbeitsgruppe Klimaforschung des Met. Inst. der Humboldt-Universität zu Berlin, **4**, 22 pp.

Roeckner, E. et al. (1992): Simulation of the present-day climate with the ECHAM model: impact of model physics and resolution. Max-Planck-Institut für Meteorologie, Report No. **93**.

Schönwiese, Ch.-D. & W. Birrong (1990): European precipitation trend statistics 1851 – 1980 including multivariate assessments of the anthropogenic CO_2 signal. *Zeitschrift für Meteorologie*, **40**, 92 – 98.

von Seggern, J. (1992): Empirische Modelle regionaler Klimaänderungen in Westeuropa und Bayern. Ph. D. thesis, University of Erlangen-Nürnberg.

von Storch, H. et al. (1993): Downscaling of Global Climatic Change Estimates to Regional Scales: an Application to Iberian Rainfall in Wintertime. *Journal of Climate*, **6**, 1161 – 1171.

Wallace, J.M. & Y. Zhang (1993): Structure and seasonality of interannual and interdecadal variability of the geopotential height and temperature fields in the northern hemisphere troposphere. *Journal of Climate*, **6**, 2063 – 2082.

Wigley, T.M.L. et al. (1990): Obtaining Sub-Grid-Scale Information from Coarse-Resolution General Circulation Model Output. *Journal of Geophysical Research*, **95** (D2), 1943 – 1953.